Effect of tunneling on ionization of Rydberg states in intense fields: Hydrogenic atoms

James S. Cohen*
Theoretical Division, Los Alamos National Laboratory, Los Alamos, New Mexico 87545, USA
(Received 8 February 2003; published 24 September 2003)

The ionization probabilities of hydrogenic Rydberg states in intense fields are calculated using a trajectory method, which was previously shown to be accurate for ionization of the ground-state hydrogen atom [J. S. Cohen, Phys. Rev. A **64**, 043412 (2001)]. It is found that the ionization probability approaches the classical over-the-barrier probability for sufficiently large n quantum numbers, but that tunneling still significantly decreases the onset field strengths at surprisingly high n. Calculations are done for ns, np_0, and $np_\pm$ targets, subjected to sudden and adiabatically ramped pulses in the long-wavelength limit. The dependence on the angular-momentum projection m along the field axis is also examined for circular orbits.

DOI: 10.1103/PhysRevA.68.033409 PACS number(s): 32.80.Rm, 02.70.Ns

I. INTRODUCTION

Field ionization has proved to be a useful tool for detecting the state of Rydberg atoms [1,2]. The accuracy of this technique depends on reliable theoretical characterization of the behavior at field strengths where the ionization becomes measurable. For the ground state, intense-field ionization is dominated by tunneling, and ionization is essentially complete before the classical threshold is reached if the pulse is adiabatically ramped. Actually, almost any experimental pulse presently achievable [3] will be near adiabatic for the ground-state hydrogen atom. On the contrary, for very high n, most pulses will be sudden (compared with the orbital period), and, by the correspondence principle, the sharp classical threshold is expected to apply.

However, for purely hydrogenic states, there is an additional symmetry, which prevents some fraction of states from ionizing at that threshold; some states may ionize only at much higher field strengths [4,5]. The states can be characterized by parabolic quantum numbers [6] n_1,n_2,m (separation parameters classically), but it is most useful to present results for states in polar coordinates n,l,m since this is the way the atom is normally prepared [7]. As the field is turned on, the states of (n,l,m) are projected on states of (n_1,n_2,m). The results of this projection depend on how the field is turned on. Hydrogenic states of given n but different l (or n_1,n_2) and m are degenerate in the absence of an external field but split and mixed by a field (in a field linearly polarized along the quantization axis, m is conserved). Thus the ionization cannot be characterized by a simple rate. We will circumvent this problem by presenting ionization probabilities at short and long times.

We recently showed that accurate rates for ionization of the ground-state hydrogen atom are obtained using the classical-trajectory Monte Carlo (CTMC) method with allowance for tunneling at the classical turning points [8]. In this method, over-the-barrier and tunneling ionization [9] are treated self-consistently. The CTMC method is valid in the high-n limit [10] and has previously been used for intense-field ionization of such states [11]. The purpose of the present work is to investigate intermediate n and the transition in behavior from mainly tunneling at low n to mainly over-the-barrier ionization at high n.

In the absence of a finite core, the energies (more precisely, actions) in coordinates $\xi\ (=r+z)$ and $\eta\ (=r-z)$ do not couple. The potential in one of the coordinates, say ξ for a given sign of the field, goes to ∞ as $\xi\rightarrow\infty$ and the motion is bound, whereas the motion in the other coordinate η is unbound or faces a barrier, depending on the magnitude of the field. If the energy in the η direction is less than the barrier height, tunneling is required for ionization to occur.

If the energy is sufficient to surmount the barrier, then ionization occurs in the time scale of classical oscillation of the angular momentum $0<l<n$. The variation in l corresponds to the changing eccentricity and orientation of the elliptical orbit [12]. Such oscillation occurs even for the purely hydrogenic states (at frequency $3nF$ in a.u. [13]), but such that the partitioning between the ξ and η degrees of freedom is unaffected. That is, (n,l) varies, but in such a fashion that the projections of the actions (n,l,m), which are good quantum numbers in the absence of a field, on the parabolic action variables I_η, I_ξ, and I_ϕ are conserved ($I_\phi=m$ in a linearly polarized field [11]). For the hydrogenic Rydberg state, the orbital axis (Runge-Lenz vector) does not precess. This stabilizing effect, manifested by the parabolic separability, is essentially the same classically and quantum mechanically. For classically stable orbits, tunneling determines the time scale for ionization.

We are concerned in this paper with the combined effects of tunneling and classical stability, in particular for ns, np_0, and $np_\pm$ states, which are reachable from the ground state by allowed optical excitation and most used experimentally. We determine the values of n and m for which a purely classical treatment suffices. The calculations are done with a dc field. In the long-wavelength region, the ac rates can be evaluated by convoluting the dc rates with the ac time dependence of the pulse. The ac results are expected to approach the cycle-averaged dc results as the frequency decreases or the field strength increases [14].

II. METHOD

The method is essentially the same as previously used for ionization of the ground-state hydrogen atom in an intense

*Electronic address: cohen@lanl.gov

field [8], except that a dc field is used. As is well known and demonstrated in that work, atomic ionization by strong low-frequency ($\omega \ll n^{-3}$ in a.u.) radiation closely resembles static-field ionization and the critical field strengths are the same [14]. Accordingly we use the field[1]

$$F(t)=\begin{cases} 0 & \text{for } t\leqslant 0, \\ F_0 \sin^2(\pi t/2\tau)\hat{z} & \text{for } 0<t<\tau, \\ F_0\hat{z} & \text{for } t\geqslant \tau. \end{cases} \tag{1}$$

Numerically exact classical dynamics is performed with Monte Carlo initial conditions. These initial conditions are randomly sampled from the uniform phase space satisfying $E=-1/2n^2$, with fixed angular momentum l and projection m on the z axis.

In the case of $l=0$, it is actually necessary to use a small nonzero value to avoid the nuclear singularity. It was found that this value could be chosen small enough that the results were quite insensitive to it. On the other hand, it was found that avoiding the nuclear singularity by introducing a small core was completely unacceptable because it destroys the special Coulomb symmetry and causes truly stable orbitals to ionize. Any core large enough to avoid numerical problems, associated with the singularity, was found to lead to this *physical* instability.[2]

Tunneling in the field direction is allowed at classical turning points using the JWKB approximation. Unlike the case of a central potential, neither the classical turning points nor the path of integration are uniquely prescribed by the usual JWKB theory. We make the intuitive assumption that tunneling occurs in the direction of the external field, starting from a classical turning point in that direction. Thus the tunneling integral is done from $\boldsymbol{r}_c$, a point in the trajectory where $dz/dt=0$ and $-\boldsymbol{F}\cdot\boldsymbol{r}>0$, in the direction $\hat{z}$ to a point $\boldsymbol{r}_c+\zeta_0\hat{\boldsymbol{z}}$ where $V(\boldsymbol{r}_c+\zeta_0\hat{\boldsymbol{z}})=V(\boldsymbol{r}_c)$. Every time these conditions are satisfied the tunneling probability is calculated by

$$P_{\text{tun}}=\exp\left\{-2(2\mu)^{1/2}\int_0^{\zeta_0}[V(\boldsymbol{r}_c+\zeta\hat{\boldsymbol{z}})-V(\boldsymbol{r}_c)]^{1/2}d\zeta\right\}, \tag{2}$$

where μ is the reduced mass of the electron. If this probability is greater than a random number in $(0,1)$, tunneling is deemed to have occurred and the trajectory is continued classically at the point $\boldsymbol{r}_c+\zeta_0\hat{\boldsymbol{z}}$. Otherwise the trajectory continues unaltered.

In the case of an $l=0$ orbit near the z axis, this tunneling path is through the saddle point and the obvious choice. In other situations the choice is not so clear-cut, but, on the average for turning points at various places on the equipotential surface, seems reasonable. Still this choice may not be optimal and deserves further investigation. The tunneling is assumed to occur instantaneously. Since the field is taken to be dc there is no possibility for tunneling back and ionization is irreversible.

We are most concerned in the present work with the change in behavior as the principal quantum number n increases. Using reduced variables helps put things in perspective. The effective potential[3] for the hydrogenic atom in a field is

$$V=\frac{m^2}{2\mu\rho^2}-\frac{Ze^2}{r}+Fz, \tag{3}$$

where ρ is the cylindrical coordinate and $r=(\rho^2+z^2)^{1/2}$. The classical equations of motion are invariant under the transformations [10,15]

$$\text{distance } r\rightarrow rn^2/Z, \tag{4a}$$

$$\text{momentum } p\rightarrow pZ/n, \tag{4b}$$

$$\text{time } t\rightarrow tn^3/Z^2, \tag{4c}$$

$$\text{field strength } F\rightarrow FZ^3/n^4, \tag{4d}$$

$$\text{potential energy } V\rightarrow VZ^2/n^2, \tag{4e}$$

$$\text{angular momentum } l\rightarrow ln, \tag{4f}$$

and

$$\text{angular momentum projection } m\rightarrow mn. \tag{4g}$$

Equipotential contours are shown in Fig. 1(a) for $m=0$, in terms of the reduced variables of Eq. (4). The potential is drawn in the y-z plane but is really a symmetric surface of revolution about the z axis. The solid polarized circle shows the outer limits of the classical ground-state motion where $V=-0.5$ a.u. and the kinetic energy is zero. The distortion is due to the Stark interaction with a field of 0.05 a.u., linearly polarized in the z direction. The classical turning point will be inside the distorted circle (sphere in three dimensions).

The solid curve to the right shows where the potential is again -0.5 a.u. To get from one to the other requires tunneling through regions of higher potential indicated by the dashed contours. The highest tunneling probability would be achieved along the z axis through the saddle point, which is located at

[1]We take the quantization axis and field polarization direction to be $\hat{z}$ instead of $\hat{x}$ as used in Ref. [8]. Atomic units ($\hbar=e=m_e$) or reduced units [see Eq. (4)] are used.

[2]This problem is treated in a future work, dealing with nonhydrogenic Rydberg atoms.

[3]This is the radial potential with centrifugal term. The actual numerical calculations are done in three dimensions in the laboratory frame.

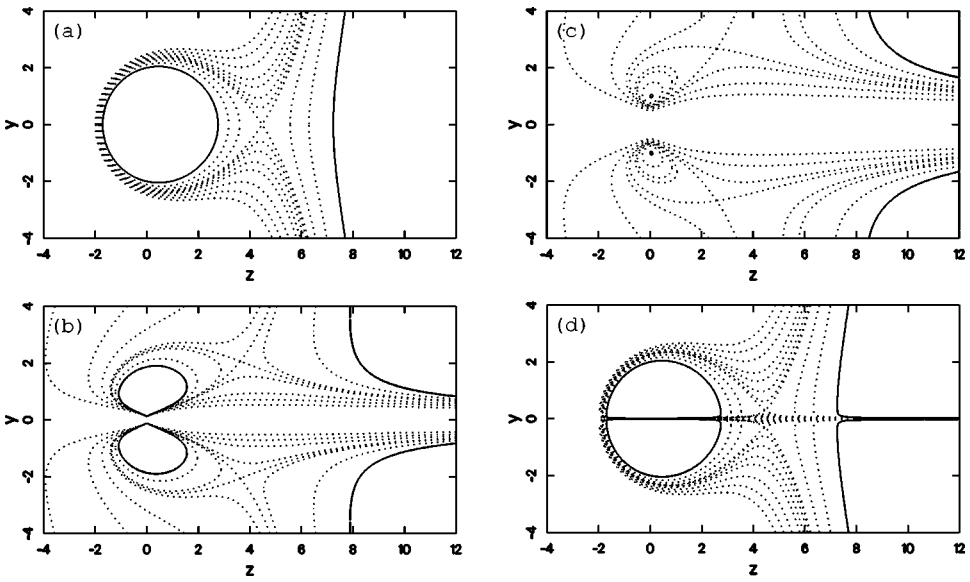

FIG. 1. Equipotential contours of Eq. (3) with $Z=\mu=1$ and $F=0.05/n^4$ a.u., shown in the y-z plane. The contours are actually surfaces of revolution about the z axes. The units of the y and z axis are n^2a_0 and energy units are $1/n^2$ a.u. In all cases the solid curves correspond to $V=-0.5$. The cases shown are (a) $m=0$, with contours at -0.500, -0.474, -0.458, -0.4472 (saddle point), -0.445, -0.442, -0.437, -0.432, -0.422, -0.412, and -0.402; (b) $m=\pm 0.5n$, with contours at 0.500, -0.450, -0.400, -0.3916 (saddle point), -0.380, -0.300, -0.200, and 0.0; (c) $m=\pm n$, with contours at -0.500, -0.450, -0.400, -0.380, -0.3282 (saddle point), -0.300, -0.200, and 0.0; (d) $m=0.01n$, with contours at -0.500, -0.474, -0.458, -0.4462 (saddle point), -0.445, -0.442, -0.437, -0.432, -0.422, -0.412, and -0.402.

$$z_{\text{saddle}}=1/\sqrt{F}=4.47, \tag{5}$$

with

$$V_{\text{saddle}}=-\frac{1}{z_{\text{saddle}}}-Fz_{\text{saddle}}=-0.447 \tag{6}$$

for $F=0.05$. The same plot would apply to the scaled variables, in this case $F=0.05Z^3/n^4$ and $V=-0.5Z^2/n^2$ with the y and z axes multiplied by n^2/Z. The angular momentum projected in the field direction is $m=0$, so it is still zero when scaled.

Note that the potential in Eq. (3) depends only on m and not on the total angular momentum l. This corresponds to the fact that l oscillates between $|m|$ and n ($n-1$ quantum mechanically). However, this picture does not tell the whole story for the hydrogenic Rydberg atom; it does not exhibit the dynamical effect of the spherical symmetry manifested by the Coulomb potential.

Figure 1(b) shows the equipotential contours for $m=\pm n/2$, which includes the $2p_{\pm}$ state of hydrogen. The electron is repelled from the z axis by the centrifugal potential, and the equipotential surfaces are skewed from the z axis. The saddle point lies at $z=3.61$ and $\rho=2.06$, with $V=-0.392$. Obviously, tunneling is now much more difficult than in the $m=0$ case. Figure 1(c) shows the equipotential contours for the classical $n=m$ orientation. In this case, the classical orbit is a circle in the x-y plane and thus collapses to points at $(y,z)=(\pm 1,0)$ in the figure. At $z>0$ the field of $F=0.05$ only slightly expands the orbit. The saddle point is skewed to $z=2.57$ and $\rho=2.67$ with $V=-0.328$. This $m=\pm n$ limit, which requires $l=n$, is not permitted quantum mechanically but can be closely approached by near-circular orbitals with $l=n-1$ at large n. Note that in the opposite limit, $m=\pm 1$ and large n, shown in Fig. 1(d), the equipotential surfaces look similar to those in Fig. 1(a) except for an excluded region near the z axis.

For a completely classical treatment, it is sufficient to do the dynamical calculation only for $n=1$. However, the scaling laws do not apply quantum mechanically because of the dimensions of $\hbar$. Within the JWKB approximation, tunneling does have a (nonlinear) scaling, but it is quite different from Eq. (4). Using the scaling relations in Eq. (4) we see that

$$P_{\text{tun}}(n)=[P_{\text{tun}}(1)]^n, \tag{7}$$

which is certainly not invariant. Obviously the effect of tunneling goes to zero as $n\to\infty$ since $P_{\text{tun}}(1)<1$. However, the value of $P_{\text{tun}}(1)$ is generally different for each trajectory, so there is no simple scaling for the total ionization probability at intermediate values of n.

The relative importance of tunneling is most easily seen by plotting the ionization probability as a function of the reduced field strength,

$$F_r=n^4F. \tag{8}$$

This is completely clear for $l=0$ (ns states) since the reduced plots would be identical in the absence of tunneling. For the np states, the comparison is not quite so clear-cut since we do not want to scale l and m as required for strict classical

invariance. As shown previously [8], the best results are obtained using initial $l=0$ for the s state, rather than $0<l<n$ as often used in CTMC calculations. The initial energies are the exact energies of the Rydberg levels.

Another important consideration is the rise time τ of the pulse in Eq. (1). As shown in Ref. [8], the ionization probability can depend drastically on the rise time. The pulse is adiabatic if the rise occurs over many periods of the classical orbit, and sudden in the opposite limit. (This is similar to the long-wavelength criterion $\omega \ll n^{-3}$.) We used $\tau=0$ for the sudden case and $\tau=50n^3$ for the adiabatic case. Thus τ is also scaled as n^3. The rise time of $50n^3$ a.u. corresponds to $50/\pi \approx 16$ classical orbits, which was found sufficient to achieve nearly adiabatic behavior. We will present results at $50n^3$ a.u. after the pulse reaches its full intensity, thus at $t=50n^3$ for the sudden pulse and $t=100n^3$ for the adiabatic pulse, as well as results at long time. A (scaled) time of $\sim 10^4 n^3$ was generally found long enough to characterize the long-time classical probabilities. Of course, in principle, complete ionization would be attained in any case at infinite time with allowance for tunneling.

The Monte Carlo trajectory method used in this work has statistical errors associated with the calculated quantities. For the sake of clarity, these error bars are not shown in the figures. While a detailed discussion of the statistics is unnecessary, an estimate of the associated uncertainties is easy to obtain. The fractional standard deviation is given by

$$\frac{\Delta P}{P}=\left(\frac{1-P}{PN}\right)^{1/2}, \tag{9}$$

where P is the fraction of N total tries in which the event occurred. For the ionization probabilities, N is the number of trajectories, generally 1000. For tunneling, N is the number of times classical turning points are reached, which is generally many times per trajectory.

III. RESULTS

A. Ionization of zero-angular-momentum (*ns*) states

The probability of ionization in an intense field can depend greatly on how the pulse is turned on. Classically, this effect is brought about by the dependence of the energy gained from the field on the initial position of the electron [8]. Although the average energy imparted may be similar for sudden or adiabatic imposition of a given field, the range of energies is not. This effect can be discussed in terms of the parameter α in Kepler's equation [15], which gives the position $0 \leqslant \alpha \leqslant 2\pi$ in the unperturbed orbital proportional to time. The adiabatic result is independent of the phase α, while the sudden result has a minimum and maximum ionization probability as a function of α. The maximum determines the threshold, so generally the ionization threshold is lower with a sudden pulse, although the sudden ionization probability is not necessarily greater than the adiabatic probability at higher field strengths.

This effect can be seen in Figs. 2 and 3 for *ns* hydrogen atoms subjected to sudden and adiabatic pulses, respectively.

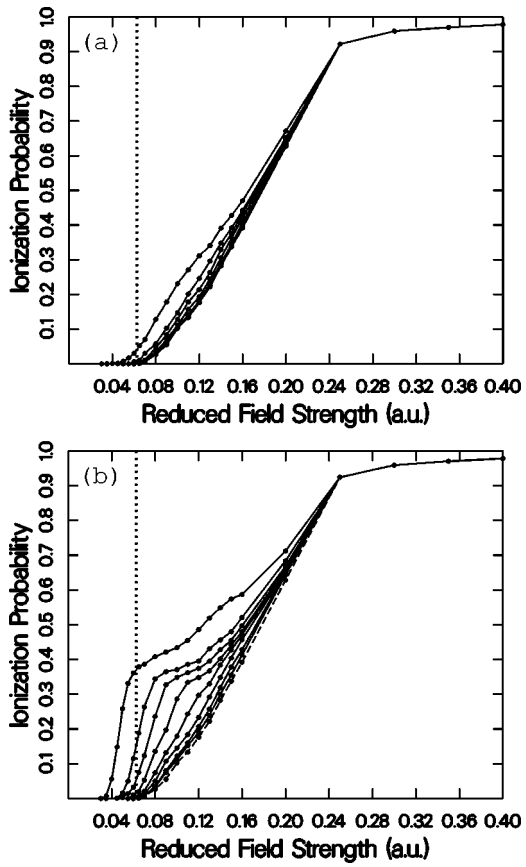

FIG. 2. Ionization probabilities for *ns* states of the hydrogen atom as a function of reduced field strength (in units of $1/n^4$ a.u.) for a sudden dc field at times of (a) $50n^3$ a.u. and (b) $5000n^3$ a.u. The solid curves from highest to lowest are for $n=1$, 2, 3, 5, 10, 20, 50, and 100. The dashed curve is the purely classical result, which is independent of n in these reduced units. The data points indicate where calculations were done and are connected by straight line segments. The vertical dotted line shows the classical threshold.

Parts (a) of the figures give the ionization probability at a time that is early but sufficiently long for a pulse to achieve full intensity adiabatically. Parts (b) give the ionization probabilities at a long time.

First we will discuss the purely classical calculation (no tunneling). Note that essentially all the ionization seen at the late time has already occurred at the early time. Sample calculations were continued to much longer times ($10^5 n^3$ a.u.) and no more ionization occurred classically. Thus what is really seen here is not the result of a time-independent rate, but rather the fraction of orbits that are subject to classical ionization at a given field strength. The ionization then occurs in a time on the order of an orbital period.

As shown in Ref. [8], the classical threshold for ionization by a sudden pulse is $0.0625/n^4$, and the threshold for ionization by an adiabatic pulse is $0.130/n^4$. These thresholds are exhibited in Figs. 2 and 3. The classical cross section is zero at threshold and small just above threshold because most trajectories miss the saddle point. The adiabatic ionization probability rises much more rapidly just above threshold and the two values are comparable at $F_r \approx 0.15$. Even at $F_r=0.3$, well above threshold, ionization is still not complete.

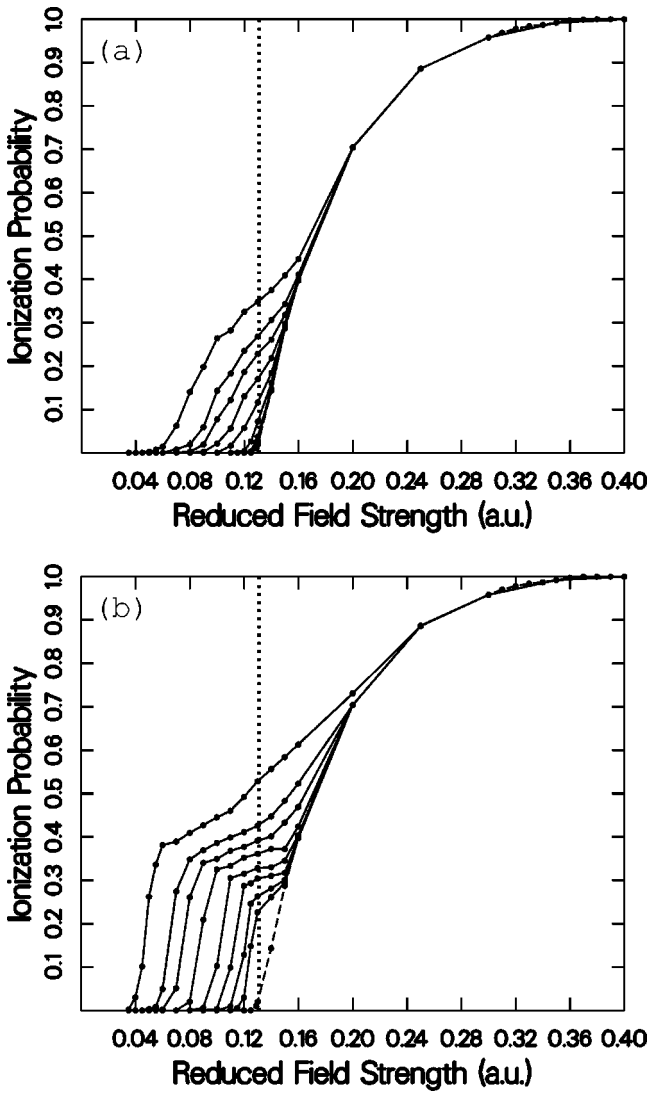

FIG. 3. Same as Fig. 2 except for a near-adiabatic pulse and with the time in part (a) $50n^3$ a.u. after the rise time of $50n^3$ a.u.

At still higher field strengths the magnitudes of the two ionization probabilities are reversed. In the case of the adiabatic pulse, ionization is complete at $F_r \approx 0.40$. However, in the case of the sudden pulse, the ionization probability approaches unity only asymptotically as $F_r \to \infty$.

The near-threshold and asymptotic behaviors for ionization by a sudden pulse have basically the same explanation. Both correspond to $l=0$ orbits aligned with the z axis with the pulse turned on when the electron is near the nucleus (perigee of the orbit); threshold occurs when the apogee is on the field-favored side of the nucleus and asymptote when the apogee is on the unfavored side of the nucleus. These cases correspond to blue- and redshifted states, respectively. The redshifted levels from state n cross the blueshifted levels from state $n+1$, but are uncoupled in hydrogenic atoms. Note that this high-field behavior is somewhat of an artifact of the dc field; in an ac field the favored and unfavored sides alternate with the sign of the field. These situations do not occur with adiabatic excitation since the electron traverses its full orbit at every field strength during the adiabatic rise.

Now we turn to the effect of tunneling. Comparison of parts (a) and (b) of Figs. 2 and 3 shows that most classical ionization occurs after only a few periods of motion, while the tunneling contribution occurs at longer times. In very strong fields, $F_r \gtrsim 0.3$, the effect of tunneling is negligible even for the $1s$ state; i.e., all ionization occurs by the over-the-barrier mechanism. Calculations for $n=1000$ (not shown) gave results differing from the purely classical results only very close to threshold. However, tunneling is still important at surprisingly high n, e.g., $n=100$ shown in Figs. 2 and 3, more so with the adiabatic pulse than with the sudden pulse. In these cases tunneling overwhelms the classical saddle-point behavior. For lower n, tunneling greatly reduces the difference between the adiabatic and sudden results. The field strengths at which ionization becomes significant (strictly speaking, there is no threshold) are only modestly higher for the adiabatic pulse than for the sudden pulse in the cases of $n \leqslant 5$. This shows that the adiabatic pulse tends to put electrons below the classical threshold into orbits having high tunneling probabilities.

The ionization probabilities display multiple slopes as a function of field strength. The reason for this behavior is similar to the reason that a single rate cannot characterize the ionization at a given field strength. Some classes of orbitals tunnel more easily than others; when they are depleted, tunneling proceeds more slowly with the next class. Some orbitals face such a large barrier to tunneling that they are almost as persistent as the purely classical orbit.

Figures 4 and 5 show the average tunneling probabilities and the fraction of ionizations that resulted from tunneling. The average tunneling probability is given by the fraction of tunneling attempts that resulted in tunneling, summed over all trajectories. Since tunneling is generally more difficult in the long-lived trajectories, this measure of average probability depends somewhat on how long the trajectories are run. As already evident from the ionization probabilities in Figs. 2 and 3, the tunneling probabilities decrease with increasing n as high as 1000. As a function of field strength, the tunneling probabilities increase rapidly at the onset and are then fairly flat at moderate field strengths.

Below the classical threshold, ionization can come only via tunneling, but even above the classical threshold tunneling can still be seen to be important. Tunneling may be the only ionization mechanism for orbitals that are stable by virtue of the special hydrogenic symmetry. However, it is also possible for an orbital that would eventually reach a classical opening to tunnel before that.

The fractions of ionizations resulting from tunneling depend on the pulse shape. In the adiabatic case [Fig. 5(b)] below the classical adiabatic threshold, it is obvious that ionization can come only by tunneling; here tunneling is very effective. It is interesting that, above the much lower sudden threshold, tunneling still accounts for a large fraction of the ionizations. This is because many of the suddenly excited orbitals do not find the classical opening. There are two clearly separated contributions to ionization, the first occurring almost instantly—within a few orbital periods of the excitation—followed by slower, delayed contributions.

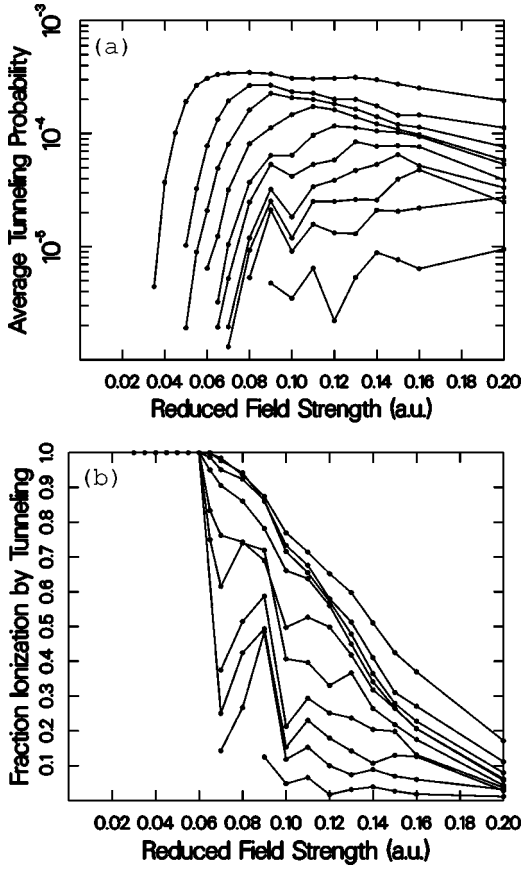

FIG. 4. (a) Average tunneling probability and (b) fraction of ionizations occurring via tunneling corresponding to the sudden ionization probabilities shown in Fig. 2(b). The curves from highest to lowest are for $n=1$, 2, 3, 5, 10, 20, 50, 100, 200, and 1000 (the last two not shown in Fig. 2). Some fluctuations in the values as a function of field strength at the higher n may be statistical due to the relatively few tunneling events in these nearly classical orbitals. The number of tunneling *attempts* at each point shown is typically $\sim 10^6$ (somewhat higher below the classical threshold and lower above the threshold).

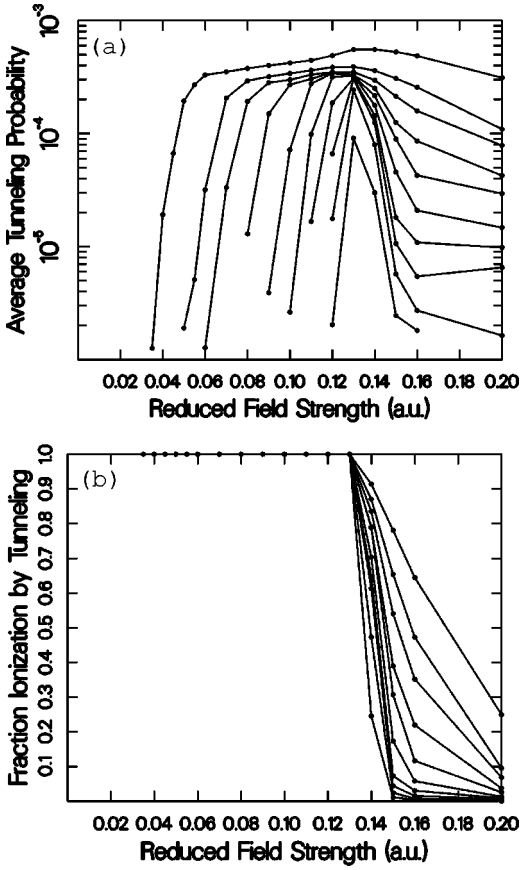

FIG. 5. (a) Average tunneling probability and (b) fraction of ionizations occurring via tunneling corresponding to the near-adiabatic ionization probabilities shown in Fig. 3(b). The curves from highest to lowest are for $n=1$, 2, 3, 5, 10, 20, 50, 100, 200, and 1000 (the last two not shown in Fig. 3). The number of tunneling *attempts* at each point shown is typically $\sim 10^6$.

B. Ionization of np_0 states

The ionization probabilities for np_0 states of hydrogen, with $n=2$, 10, and 100, are shown in Figs. 6 and 7 for sudden and adiabatic pulses, respectively. Their behavior is similar to that of the *ns* states ($n \geqslant 2$)—a little higher at low field strengths and a little lower at high field strengths. This relative insensitivity to l is a result of l oscillating between 0 and n due to the field. However, due to the Coulomb symmetry, this motion is not ergodic and there are still significant differences between the *ns* and np_0 results.

Unlike the *ns* state, the classical results (dashed curves) do not trivially scale with n and are not the same in terms of the reduced field strength, although scaling invariance is reached for large n since in this limit $l/n \rightarrow 0$.

C. Ionization of $np_\pm$ states

The results for $np_\pm$ states are shown in Figs. 8 and 9 for the sudden and adiabatic pulses, respectively. The component of angular momentum $|m|=1$ along the field axis is conserved and increases the classical threshold for ionization [16–18]. Although the classical values for fixed m do not strictly scale with F_r, they are not very different and only the curve for $n=2$ is shown. States of higher $|m|$ have higher ionization thresholds since a portion of their kinetic energy is required for motion perpendicular to the field [19]. The centrifugal barrier also greatly reduces the effectiveness of tunneling. It can be seen in the figures that the onset for ionization for the $2p_\pm$ state is moderately depressed by tunneling. While the tunneling path chosen in this calculation may not be optimal, it is not expected to affect this conclusion.

The greatest source of differences between the results of sudden and adiabatic excitation has a classical origin. Ionization with an adiabatic pulse can be seen in Fig. 9 to occur rather sharply at a field strength of $\sim 0.16/n^4$ a.u. In the case of sudden excitation, about half of the atoms are ionized at this field strength, but the onset is considerably lower and saturation much higher.

D. Dependence on m in circular orbits

In this section we will examine the effect of the angular-momentum component m along the field axis in more detail. By symmetry the results are independent of the sign of m.

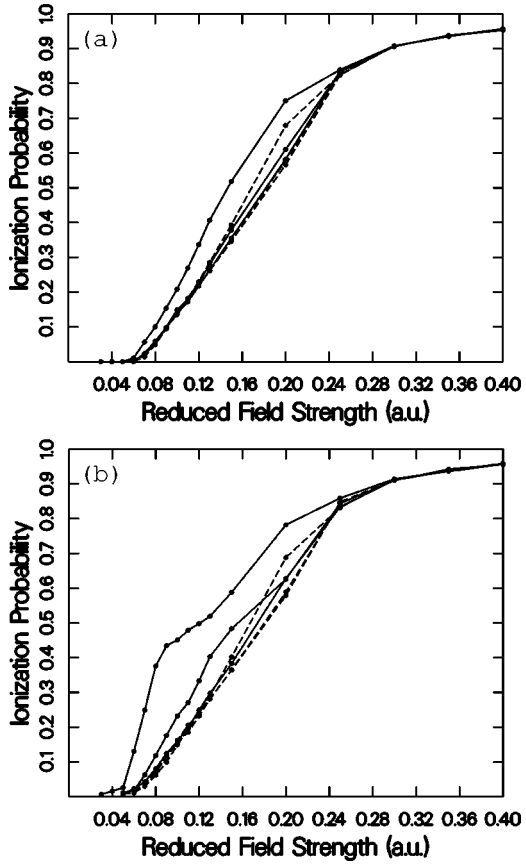

FIG. 6. Ionization probabilities for np_0 states of the hydrogen atom as a function of reduced field strength (in units of $1/n^4$ a.u.) for a sudden dc field at times of (a) $50n^3$ a.u. and (b) $5000n^3$ a.u. The solid curves from highest to lowest are for $n=2$, 10, and 100. The two dashed curves are the classical results for $n=2$ (higher) and $n=10$ and 100 (lower and almost indistinguishable). The initial angular momentum is taken to be identically 1.0, so, unlike the classical limits shown in Figs. 2 and 3, the classical limits depend slightly
on n.

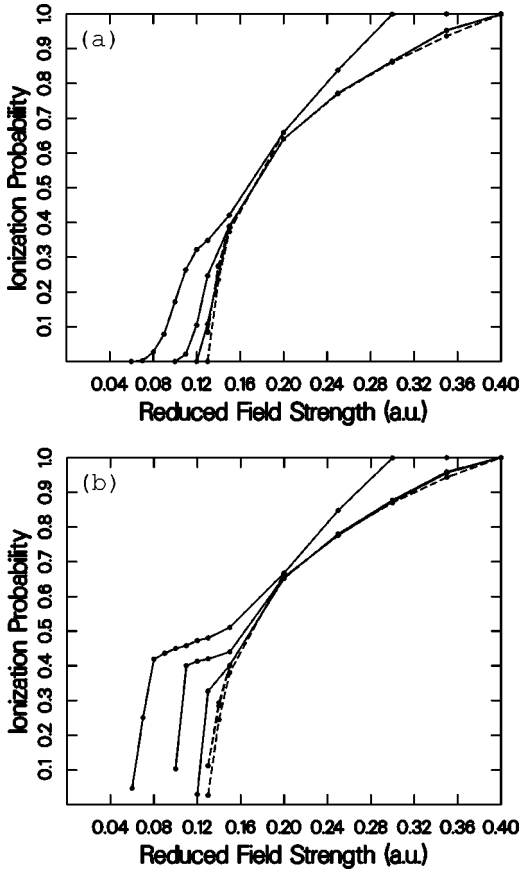

FIG. 7. Same as Fig. 6 except for a near-adiabatic pulse and with the time in part (a) $50n^3$ a.u. after the rise time of $50n^3$ a.u.

We take a near-circular orbital $n=10$, $l=9$, and consider $|m|=0$, 3, 6, and 9. The results for sudden and adiabatic pulses are shown in Figs. 10 and 11, respectively. In both cases, essentially all ionization of the $|m|=l$ orbital occurs very quickly; this shows that tunneling is very ineffective. The ionization probability goes from zero to unity over a quite narrow range of field strength. For $|m|<l$ there is significant additional ionization at later times, largely due to tunneling. In the case of the adiabatic pulse, the change is qualitative, with dramatic additional ionization at low field strengths. This diminishes, but by no means eliminates, differences due to the pulse rise time.

We also did calculations on the classical (with no quantal counterpart) state $n=l=|m|$, whose orbital is exactly circular and perpendicular to the z axis in the absence of a field. The classical ionization probability rises sharply from zero to unity, at $F_r=0.1714$ a.u. with a sudden pulse and at $F_r=0.208$ with an adiabatic pulse. It is easy to see that the classical threshold must be sharp for this special case since all points on the initial perpendicular orbit are equivalent.

With allowance for fictional tunneling, the onset of ionization (defined by $\sim 10\%$ ionized in time $t/n^3=5000$ a.u.) is reduced to $F_r \approx 0.138$ for $n=2$ and $F_r \approx 0.1704$ for $n=10$ in the sudden scenario. With an adiabatic pulse, the fictional lowering of the threshold is less, by only $\sim 10^{-4}$ for $n=2$ but a bit more (from 0.206 to 0.161) for $n=2$.

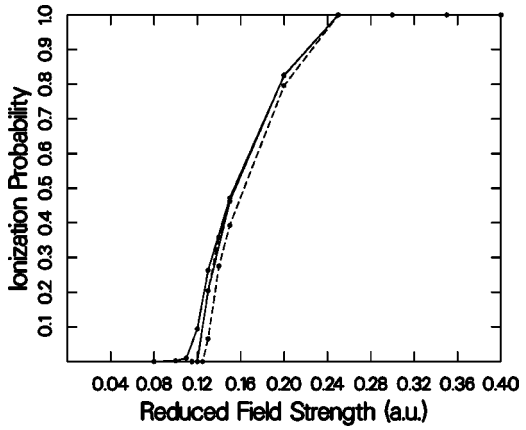

FIG. 8. Ionization probabilities for $np_{\pm}$ states of the hydrogen atom as a function of reduced field strength (in units of $1/n^4$ a.u.) for a sudden dc field after a time of $5000n^3$ a.u. The two solid curves are for $2p_{\pm}$ (higher) and $100p_{\pm}$ (lower). The dashed curve is the classical result for $2p_{\pm}$. The effect of tunneling on the $100p_{\pm}$ state is too small to be seen in this figure.

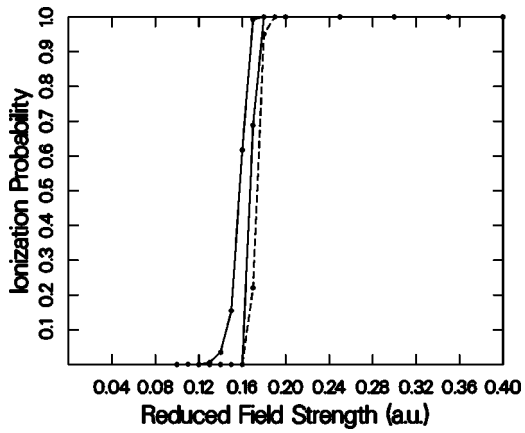

FIG. 9. Same as Fig. 8 except for near-adiabatic excitation.

IV. CONCLUSIONS

The present calculations have shown that quantum mechanical tunneling is important for intense-field ionization of hydrogenic Rydberg atoms in levels up to principal quantum number $n \approx 100$ if the state has zero projection of angular momentum ($m=0$) along the field axis. The significant onset of ionization, with probability $\gtrsim 0.1$, occurs at field strengths far below the classical threshold; the effect is more distinct for adiabatic excitation than for sudden excitation. Tunneling is still measurable in the trajectory calculations at still higher n. A significant fraction of the ionizations occur via tunneling even above the classical threshold. The role of tunneling diminishes for increasing n, which explains the experimental finding that ionization thresholds do not change much with the pulse duration for durations much longer than the Kepler period [20].

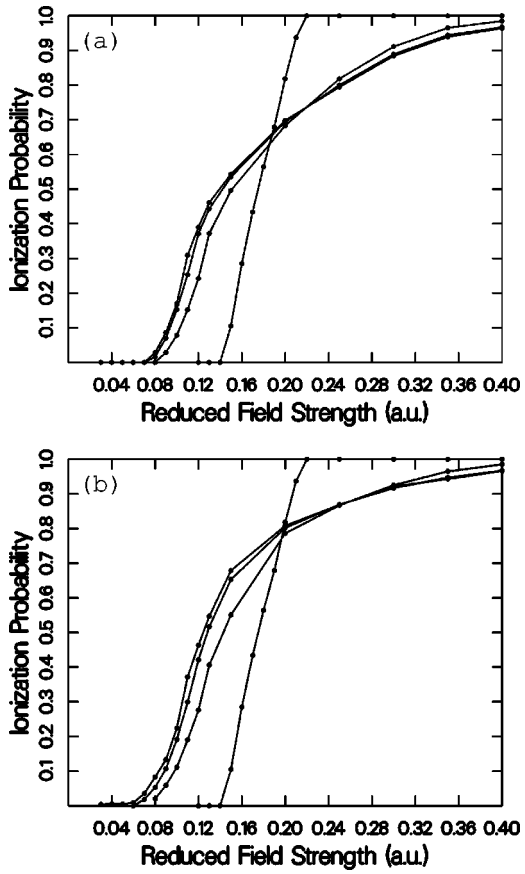

FIG. 10. Ionization probabilities for a near-circular ($n=10, l=9$) state of the hydrogen atom as a function of reduced field strength (in units of $1/n^4$ a.u.) for a sudden dc field at times of (a) $50n^3$ a.u. and (b) $5000n^3$ a.u. The curves from left to right (at low values of the ionization probability) are for angular momentum projections $|m|=0$, 3, 6, and 9.

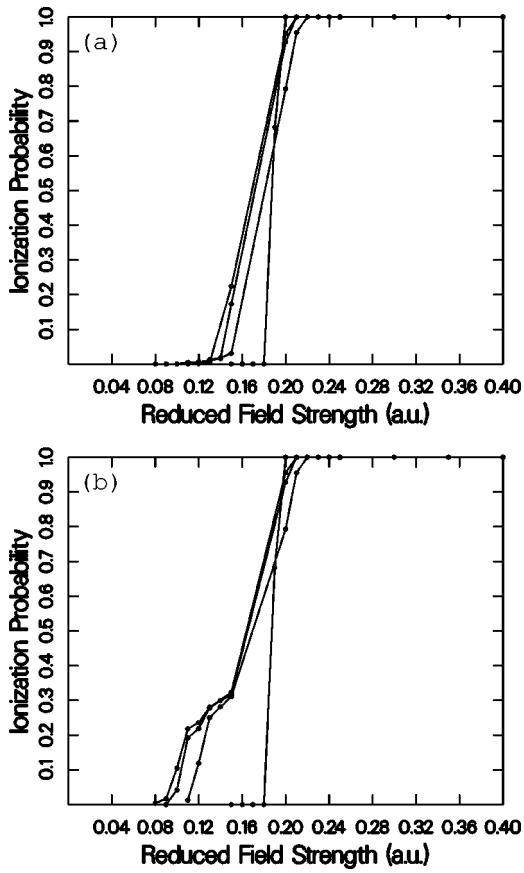

FIG. 11. Same as Fig. 10 except for a near-adiabatic pulse and with the time in part (a) $50n^3$ a.u. after the rise time of $50n^3$ a.u.

The effect of tunneling is much less for $m>0$ states. As m increases (for fixed n), the classical ionization profile becomes a sharper function of field strength. For circular orbits it becomes nearly a step function, little affected by tunneling.

Results have been presented for both sudden and adiabatic pulses. The strong dependence on the rise time is in agreement with quantum mechanical calculations [21]. While sudden excitation of the ground-state hydrogen atom is beyond present experimental capability, it is quite easy for high Rydberg states. For example, the level $n=20$ has an orbital period of about a picosecond and could be suddenly ionized by readily available femtosecond pulses. Quantum control of high Rydberg states has been achieved experimentally [22] and may offer the possibility of a direct measurement of tunneling probability in an atom.

It is important to note that the calculations in this paper apply to pure hydrogenic states. The special Coulomb symmetry, apposite in this case, can have a dramatic effect, e.g., greatly increasing the classical threshold for ionization of some states and reducing the probability of tunneling. The presence of core electrons destroys the symmetry. In future work [23], we will examine tunneling for nonhydrogenic atomic Rydberg states and address the question of how big the principal quantum number n must be for the state to behave like its hydrogenic counterpart.

ACKNOWLEDGMENTS

I am grateful to Kenneth LaGattuta for helpful comments. This work was performed under the auspices of the U.S. Department of Energy.

[1] E. Luc-Koenig and A. Bachelier, J. Phys. B **13**, 1743 (1980).
[2] T.F. Gallagher, *Rydberg Atoms* (Cambridge University Press, Cambridge, England, 1994), p. 85.
[3] A. Becker, L. Plaja, P. Moreno, M. Nurhuda, and F.H.M. Faisal, Phys. Rev. A **64**, 023408 (2001).
[4] H. Rottke and K.H. Welge, Phys. Rev. A **33**, 301 (1986).
[5] V.V. Kolosov, J. Phys. B **22**, 833 (1989).
[6] H.A. Bethe and E.E. Salpeter, *Quantum Mechanics of One- and Two-Electron Atoms* (Springer-Verlag, Berlin, 1957).
[7] E. Rabani, L.Ya. Baranov, R.D. Levine, and U. Even, Chem. Phys. Lett. **221**, 473 (1994).
[8] J.S. Cohen, Phys. Rev. A **64**, 043412 (2001).
[9] M.G. Littman, M.M. Kash, and D. Kleppner, Phys. Rev. Lett. **41**, 103 (1978).
[10] R. Abrines and I.C. Percival, Proc. Phys. Soc. London **88**, 861 (1966).
[11] E. Rabani, R.D. Levine, A. Mühlpfordt, and U. Even, J. Chem. Phys. **102**, 1619 (1995).
[12] A. ten Wolde, L.D. Noordam, A. Lagendijk, and H.B. van Linden van den Heuvell, Phys. Rev. A **40**, 485 (1989).
[13] D. Kleppner, M.G. Littman, and M.L. Zimmerman, in *Rydberg States of Atoms and Molecules*, edited by R. F. Stebbings and F. B. Dunning (Cambridge University Press, Cambridge, England, 1983), p. 73.
[14] R. Shakeshaft, R.M. Potvliege, M. Dörr, and W.E. Cooke, Phys. Rev. A **42**, 1656 (1990).
[15] L.D. Landau and E.M. Lifshitz, *Mechanics*, 3rd ed. (Pergamon, Oxford, 1976), pp. 35–39.
[16] W. van de Water, D.R. Mariani, and P.M. Koch, Phys. Rev. A **30**, 2399 (1984).
[17] D.A. Harmin, Phys. Rev. A **30**, 2413 (1984).
[18] R.G. Rolfes, L.G. Gray, and K.B. MacAdam, J. Phys. B **25**, 2319 (1992).
[19] W.E. Cooke and T.F. Gallagher, Phys. Rev. A **17**, 1226 (1978).
[20] P. Kristensen, G.M. Lankhuijzen, and L.D. Noordam, J. Phys. B **30**, 1481 (1997).
[21] S. Yoshida, C.O. Reinhold, J. Burgdörfer, B.E. Tannian, R.A. Popple, and F.B. Dunning, Phys. Rev. A **58**, 2229 (1998).
[22] B.E. Tannian, C.L. Stokely, F.B. Dunning, C.O. Reinhold, S. Yoshida, and J. Burgdörfer, Phys. Rev. A **62**, 043402 (2000).
[23] J.S. Cohen (unpublished).